iJRASET
International Journal For Research in Applied Science and Engineering Technology

# INTERNATIONAL JOURNAL FOR RESEARCH

IN APPLIED SCIENCE & ENGINEERING TECHNOLOGY

**Volume:** 5 **Issue:** XI **Month of publication:** November 2017

**DOI:**

www.ijraset.com

Call: 08813907089 | E-mail ID: ijraset@gmail.com

International Journal for Research in Applied Science & Engineering Technology (IJRASET)
*ISSN: 2321-9653; IC Value: 45.98; SJ Impact Factor:6.887*
*Volume 5 Issue XI November 2017- Available at www.ijraset.com*

# Noval $Zn_2SnO_4$-Doped $TiO_2$ Photoanode for Dye-Sensitized Solar Cells

Mogali[1], Chaitanya[2]
[1]*Assistant Professor, Department of physics, Sridevi Women's Engineering College, Vattinagulapally, Gopanpally, Hyderabad-500 075*

***Abstract:*** ***$Zn_2SnO_2$ doped $TiO_2$photo anode material general formula of (100-x) $TiO_2$+ x $Zn_2SnO_4$(x=0, 3, 5 and 7 mol%)are synthesized by simple solid-state reaction method followed by high-energy ball milling for 20 hours to form the homogeneous nano scaled photo anode material. $Zn_2SnO_4$ doped $TiO_2$photo anode shows improvement of power conversion efficiency of DSSC. Power efficiency and $Zn_2SnO_4$ nanoparticle distribution output with the increased surface area was investigated by SEM and XRD analysis.After $Zn_2SnO_4$ doping, the conductivity of the $TiO_2$ powder enhanced, and its flat-band potential ($V_{fb}$) has a positive shift. The energy-conversion efficiency of a cell based on 5.0 mol% $Zn_2SnO_4$-doped $TiO_2$ is significantly better, by about 16.1 %, compared to that of a cell based on un doped $TiO_2$.Ball milling process exhibited the best performance with optimized solar energy conversion efficiency of 8.83 % with fill factor of 0.712.***

***Keywords: Solar energy, Dye-sensitized solar cells (DSSC), $Zn_2SnO_4$ doped $TiO_2$, Photo-anode, Ball milling.***

## I. INTRODUCTION

Dye-sensitized solar cells (DSSC) have been attracting much attention as alternative energy sources for the next generation solar cells due to their low production cost, the relatively high power conversion efficiency (PCE) and ecofriendly production when compared with silicon solar cells [1-2].Several photo anode materials $TiO_2$, ZnO, $SnO_2$, $Nb_2O_5$, and $SrTiO_3$ have been studied in developing high-performance DSSC, due to their wide energy band gap (Eg> 3eV), good stability against photo corrosion (transparent to the major part of the solar spectrum) and good electronic properties [3-8].Among them, pure anatase$TiO_2$ has been proven to be the best photo anode materials due to its abundance, chemical stability and excellent charge transport capability. However, pure anatase$TiO_2$ faces poor photo anode activity, low absorption in the UV spectrum, low excitation lifetimes and low amounts of dye adsorption.

In recent years, many attempts were made to overcome the limitations of $TiO_2$ by doping with metal-oxides improve the significance of $TiO_2$photoanode material activity. However, doping ZnO/SnO metal-oxides have emerged as an excellent composite for DSSCs. Semiconducting ZnO and SnOnano particles are offering high surface area, high dye adsorption capability, high chemical stability and longer electron lifetime. Bing Tan et al [9] successfully demonstrated $Zn_2SnO_4$ as photoanode for DSSC. In order to meet the excellent charge transport capability and photoelectric conversion efficiency (η), our choice of interest is to propose a new type of $Zn_2SnO_2$ doped $TiO_2$ nano composite as a photo anode material for DSSC.

In this work, we successfully demonstrated efficient improvement of DSSC by addition of $Zn_2SnO_4$ semiconductor material to $TiO_2$photo anode material. Power conversion efficiency of $TiO_2$ significantly improved by doping $Zn_2SnO_4$,due to their lower conduction band and higher electron mobility. It facilitated more efficient electron transfer from excited states of dye molecules to $Zn_2SnO_4$ doped $TiO_2$ composite through an external load. The effect of ball milling increases the surface of photoanode materials and enhanced $Zn_2SnO_4$ dispersion in $TiO_2$ matrix and the homogeneity in the hybrid composite.

## II. EXPERIMENTAL

$Zn_2SnO_4$-Doped $TiO_2$ photo anode material synthesized by taking stoichio metric ratios of analytical reagent grade $ZnCO_3$, SnO and $TiO_2$ were mixed thoroughly and ground in an agate mortar for 30 minutes to form a homogeneous mixture. Then, the mixture is placed in an alumina crucible and annealed at 700 °C for two hours in an electric furnace. Further, high energy ball milling method was used for 20 hours to form the homogeneous nano scaled photo anode powder. Each $Zn_2SnO_4$-Doped $TiO_2$ powdered sample (approximately 3 g) was added to 2 ml of absolute ethanol in a sealed container and ball milled overnight. 0.6 ml Acetic acid and a drop of Triton™ X -100 were later added to the slurry and stirred in an agate mortar until viscous enough for pasting onto fluorine doped tin oxide coated (FTO) glass (Nippon sheet glass 10-12 $\Omega sq^{-1}$) using a microscope glass edge. After drying, an active area of ~0.3 $cm^2$ was shaped in the center of the conductive glass (2 cm x 1.1 cm). Prior to pasting, the conductive glass substrates were

©IJRASET (UGC Approved Journal): All Rights are Reserved

washed 4 times using ultra sonication in soapy water, DI water, IPA and acetone for 10 min, respectively. The prepared anodes were then sintered in a furnace at 500 $^0$C for 30 min, to remove all organic additives.

The sintered electrodes were dipped in 0.5 mM N719 dye in ethanol for 12 h at room temperature and later washed with excess ethanol. Each dyed electrode was combined with a Pt-coated glass counter electrode and sandwiched with electrolyte (EL-SGE Electrolyte, DYSOL). The electrolyte was introduced by placing a drop on the active area of the photoanode. Parafilm paper, PM-996, was carefully cut and used as a spacer. A counter electrode was then placed on top of the photoanode, and the electrodes were held firmly together by crocodile clips.

The photocurrent density–voltage (J–V) measurement was tested using a Keithly 2611 Source Meter (Keithley Instruments, Inc.). The light source was an AM 1.5 solar simulator (91160A, Newport Co.). The incident light intensity was 100 mW cm$^{-2}$ calibrated with a standard Si solar cell. The tested solar cells were masked to a working area of 0.2 cm$^2$. XRD studies carried out by using PAN analytical Diffract meter B.V fitted with Cu target (both K(α1+α2) wavelengths) and Ni filter at 40 kV and 30 mA (2h range). The crystallite sizes were examined with SEM pictures (Zeiss Gemini 1530 operated at 1kV)

## III.RESULTS AND DISCUSSIONS

Fig. 1 shows the X-ray diffraction patterns of the un doped and $Zn_2SnO_4$-doped $TiO_2$ with different $Zn_2SnO_4$ contents. The broad peaks in all the $Zn_2SnO_4$-doped $TiO_2$arewell-indexed corresponding to the major crystalline phase anatase ($TiO_2$) (ICSD Collection code # 9852), structure indexed to Tetragonal/ I 41/a m d space group and minor crystalline phase Zinc Stagnate ($Zn_2SnO_4$) phase (ICSD Collection code # 24234). This broad peaks clearly indicating that the anatase nano crystalline structure is retained after doping. The diffraction peaks shift to lower theta values with increasing $Zn_2SnO_4$ content because of the larger radius of $Zn^{2+}$ (0.74 Å) and $Sn^{4+}$ (0.69 Å) compared to that of $Ti^{4+}$ (0.61 Å), in accordance with the Bragg equation: $2d\sin\theta = n\lambda$ (Fig. 1). Furthermore, the intensity of the diffraction peaks and volume of the unit cell gradually increasing with $Zn_2SnO_4$ content up to 5 mol%. According to our knowledge, this new approach creates a higher order in the $TiO_2$ nanoparticles through the $Zn_2SnO_4$ doping, which makes the particles in favor of electron transfer, resulting in an increased photocurrent. Table I shows calculated and experimental structural parameters of $Zn_2SnO_4$ doped $TiO_2$photoanode materials.

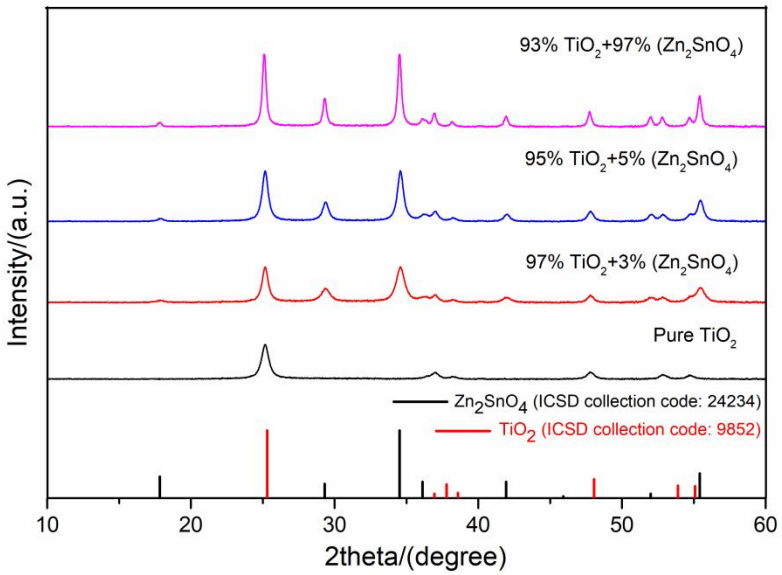


Fig. 1 XRD patterns of $Zn_2SnO_4$ -doped $TiO_2$photoanode material.

The crystallite sizes calculated from the Debye-Scherrer equation are listed in Table I, and they are shown to be well consistent with the SEM images shown in Figure 2. The SEM images in Figure 2 indicate the high crystallinity of the $TiO_2$ nanoparticles. Average crystallite size is achieved to be lowest (~ 120 nm) for 5 mol% $Zn_2SnO_4$ doped $TiO_2$ sample (Fig. 2 (c)), which clearly suggested that this sample may create the large electron-holes transfer, resulting in an increased photocurrent. Indeed, uncontrolled agglomeration $Sn^{4+}$ particles of crystallites can also be seen in the SEM image of 7 mol% $Zn_2SnO_4$ sample (Fig. 2(d)). The correlation between the microstructural and electrochemical characterization of these samples will be explained in the next section.

©IJRASET (UGC Approved Journal): All Rights are Reserved

Table I Calculated and experimental structural parameters of $TiO_2$ doped $Zn_2SnO_4$ Photo anode materials

| Photo anode material | Reference | a (Å) | b (Å) | c (Å) | α ($^0$) | β ($^0$) | γ ($^0$) | Volume [Å^3] | crystallite size (nm) | Crystal system/ Space group |
|---|---|---|---|---|---|---|---|---|---|---|
| Experimental | 10 | 3.7840 | 3.7840 | 9.5150 | 90 | 90 | 90 | 136.24 | | Tetragonal/ I 41/a m d |
| Pure $TiO_2$ | This work | 3.7795 | 3.7795 | 9.3444 | 90 | 90 | 90 | 133.48 | 200.8 nm | |
| 97% $TiO_2$ + 3% ($Zn_2SnO_4$) | This work | 3.8023 | 3.8023 | 9.7447 | 90 | 90 | 90 | 140.88 | 160.1 nm | |
| 95% $TiO_2$ + 5% ($Zn_2SnO_4$) | This work | 3.8090 | 3.8090 | 9.7327 | 90 | 90 | 90 | 141.21 | 120.4 nm | |
| 93% $TiO_2$ + 7% ($Zn_2SnO_4$) | This work | 3.7707 | 3.7707 | 9.3461 | 90 | 90 | 90 | 132.88 | 260.5 nm | |

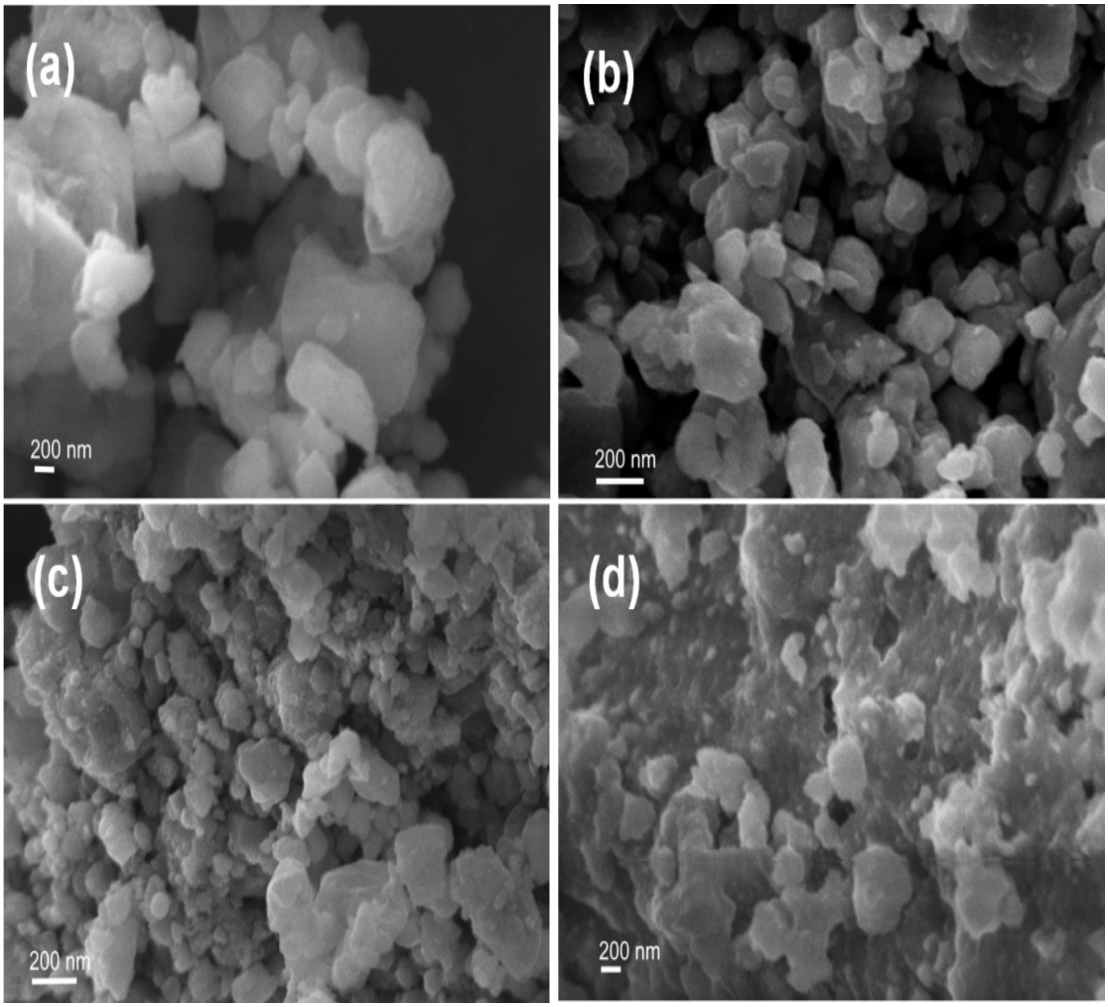


Fig. 2 SEM images of (a) un doped pure $TiO_2$ (b) 3 mol% (c) 5 mol%(d) 7 mol% $Zn_2SnO_4$ doped-$TiO_2$ photo anode materials

Fig. 3 shows average nanoparticle size distribution of SEM images (Fig. 2) of un-doped and $Zn_2SnO_4$ doped-$TiO_2$ photoanode materials by using with ImageJ software. These results clearly indicate that the crystalline size of $Zn_2SnO_4$ doped and undoped$TiO_2$ photoanode materials decreasing the crystalline size by increasing content of $Zn_2SnO_4$ up to 5 mol%. The average crystalline size is distributed to ~ 100-300 nm for all samples.

©IJRASET (UGC Approved Journal): All Rights are Reserved

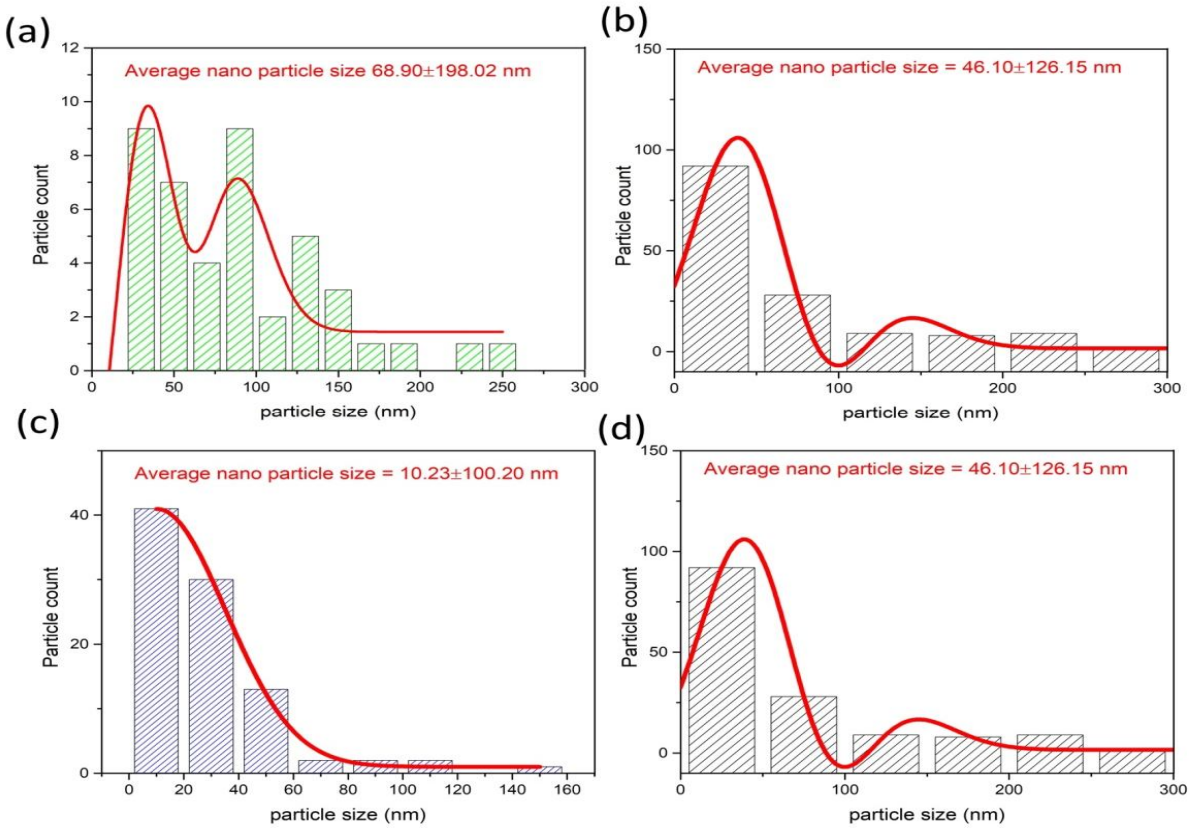


Fig. 3 Particle size distribution of (a) un doped pure $TiO_2$ (b) 3 mol% (c) 5 mol%(d) 7 mol% $Zn_2SnO_4$ doped-$TiO_2$ photoanode material SEM images.

Fig. 4 shows the current density-voltage curves of the open cells based on $Zn_2SnO_4$-doped and un doped $TiO_2$photoelectrodes. The average performance characteristics obtained from multiple cells with the same $Zn_2SnO_4$ content are summarized in Table II.The short-circuit photocurrent density ($J_{sc}$), the open-circuit voltage ($V_{OC}$) and the photoelectric conversion efficiency (η) increase with the $Zn_2SnO_4$-doping to reach a maximum at a $Zn_2SnO_4$/Ti ratio of at mol % and then decrease. The film thickness and dye-loading amount are similar for both of the photoanode films, indicating that the increase of photocurrent for the $Zn_2SnO_4$-doped $TiO_2$ is not due to the increase in the dye absorption. The higher $J_{sc}$ should result from the enhanced electron transport in the $TiO_2$ films, which could be explained in the IMPS analysis part. The higher $V_{oc}$ should result from the elevated $E_{fb}$. With the doping content increases, the concentration of impurities increases. These impurities could act as charge trapping site for the electron−hole recombination. And more serious recombination at high doping content (>5 mol %) could result in a smaller $V_{oc}$ and $J_{sc}$.

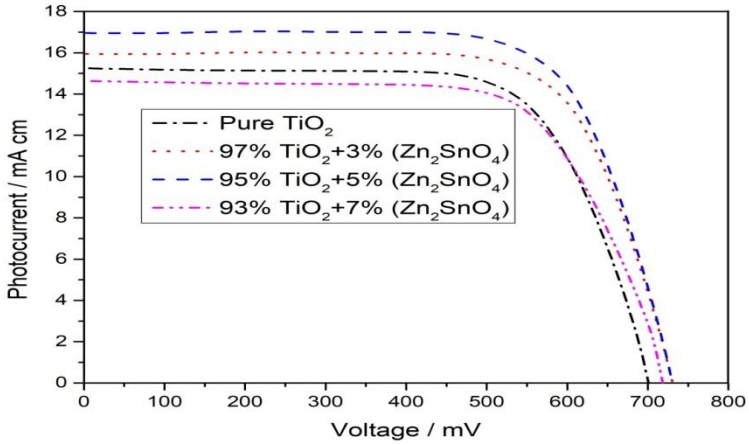


Fig. 4Current density−voltage (J−V) curves of $Zn_2SnO_4$ doped-$TiO_2$ photoanode DSSC.

©IJRASET (UGC Approved Journal): All Rights are Reserved

Table II Photovoltaic Properties of DSSC Assembled with $TiO_2$ Films of Different $Zn_2SnO_4$ Contents

| DSSC | short-circuit photocurrent ($J_{SC}$) (mA $cm^{-2}$) | open-circuit voltage ($V_{OC}$) (mV) | photoelectric conversion efficiency (η) (%) | Full fill factor (FF) | dye loading ($\times 10^{-7}$ mol $cm^{-2}$) |
|---|---|---|---|---|---|
| Pure $TiO_2$ | 15.24 | 700.64 | 7.45 | 0.697 | 0.99 |
| 97% $TiO_2$ + 3% ($Zn_2SnO_4$) | 15.94 | 730.68 | 8.32 | 0.714 | 1.02 |
| 95% $TiO_2$ + 5% ($Zn_2SnO_4$) | 16.95 | 730.68 | 8.83 | 0.712 | 0.96 |
| 93% $TiO_2$ + 7% ($Zn_2SnO_4$) | 14.63 | 718.41 | 7.24 | 0.689 | 0.97 |

EIS technique has been widely employed to investigate the kinetics of electrochemical and photo electrochemical process occurring in DSSC.As Shown in Fig. 5, the impedance spectra of DSSCs based on $TiO_2$ and $Zn_2SnO_4$-doped $TiO_2$ films were measured ranging from 1 Hz to 100 kHz. Two semicircles, including a small semicircle at high frequency and a large one at low frequency, were observed in the Nyquist plots of EIS spectra (Fig. 5). As shown in Fig. 5, the small semicircle in the frequency range (<10 Ω) fitted to a charge transfer resistance ($R_{ct}$) and the Helmholtz capacitance ($C_{\mu 1}$) should be ascribed to the charge transfer at the interfaces of the redox electrolyte/Pt counter electrode. The large semicircle in the low-frequency region fitted to a transport resistance ($R_w$) and the Helmholtz capacitance ($C_{\mu 2}$) is related to the charge transfer across either the $TiO_2$/redox electrolyte interface or the FTO/$TiO_2$ interface.

According to the EIS model fitted parameters including $R_{ct}$ and $R_w$ obtained by Z view software. Underopen circuit condition, no current passes through the external circuit, and the electrons injected into $TiO_2$ or $Zn_2SnO_4$-doped $TiO_2$ are recombined by redox electrolyte at the $TiO_2$/dye/electrolyte interface. The increased charge recombination found for the $Zn_2SnO_4$-doped $TiO_2$ cell could be attributed to higher concentration impurities due to the doping, which acts as a charge trapping site for the electron−hole recombination, hence leading to the decreasing of photon-to-electron conversion efficiency at high $Zn_2SnO_4$content (>5 mol %). The Helmholtz capacitance describes the change of electron density under a small variation of the Fermi level. Thus, the value of $C_{\mu 2}$ gives the total density of free electrons in the $TiO_2$ conduction band and localized electrons in the trap states. The $Zn_2SnO_4$-doped $TiO_2$ film had a smaller capacitance value than the pure-$TiO_2$film, whichresults from the fact that less photogenerated electrons are captured by the empty trap states in the $Zn_2SnO_4$-doped film due to doping, and this result favors the electron transport.

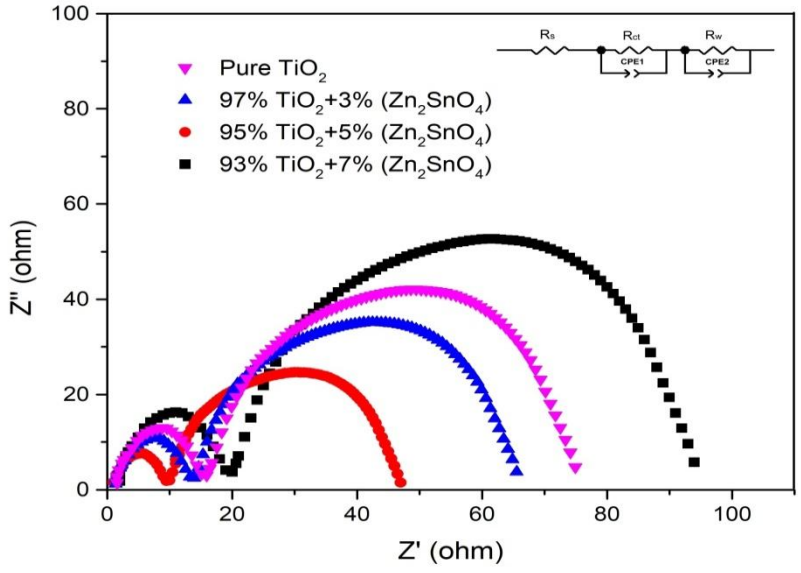


Fig. 5 EIS spectra of the $TiO_2$ and the $Zn_2SnO_4$-doped $TiO_2$ DSSC

©IJRASET (UGC Approved Journal): All Rights are Reserved

## IV. CONCLUSION

In summary, the $Zn_2SnO_4$-doped $TiO_2$ were successfully prepared by simple solid-state reaction method followed by high-energy ball milling under optimized $Zn_2SnO_4$ content. The best efficiency of 8.83% was achieved by DSSC with 5 mol % $Zn_2SnO_4$ -doped $TiO_2$, which gave an efficiency improved by 16.1% compared with that of the cells based on pure $TiO_2$. The DSSC with $Zn_2SnO_4$-doped $TiO_2$was found to improve the open circuit voltage due to the negative shift of $V_{fb}$ of $TiO_2$ and enhance the short-circuit current density due to the faster electron transport in the $Zn_2SnO_4$-doped $TiO_2$ films. EIS measurement indicates that the increased charge recombination found for the $Zn_2SnO_4$-doped $TiO_2$ cell could be attributed to high concentration impurities due to the doping, which acts as charge trapping site for the electron−hole recombination, hence leading to the decreasing of photon-to-electron conversion efficiency at the high $Zn_2SnO_4$ content (>5 mol %). These findings pave a new way to tune the band structure of $TiO_2$ and improve the charge transport for the high performance of DSSC. Therefore, $Zn_2SnO_4$-doped $TiO_2$ may be developed as a promising photo electrode material for high-efficiency DSSC and other phothoenergy conversion devices.

## REFERENCES

[1] L. El Chaar and N. El Zein, "Review of photovoltaic technologies," *Renewable and sustainable energy reviews,* vol. 15, pp. 2165-2175, 2011.
[2] B. O'regan and M. Grätzel, "A low-cost, high-efficiency solar cell based on dye-sensitized colloidal $TiO_2$ films," *nature,* vol. 353, pp. 737-740, 1991.
[3] M. K. Nazeeruddin, F. De Angelis, S. Fantacci, A. Selloni, G. Viscardi, P. Liska, *et al.*, "Combined experimental and DFT-TDDFT computational study of photoelectrochemical cell ruthenium sensitizers," *Journal of the American Chemical Society,* vol. 127, pp. 16835-16847, 2005.
[4] V. Kumar, N. Singh, V. Kumar, L. Purohit, A. Kapoor, O. M. Ntwaeaborwa, *et al*., "Doped zinc oxide window layers for dye-sensitized solar cells," *Journal of Applied Physics,* vol. 114, p. 134506, 2013.
[5] R. A. Jensen, H. Van Ryswyk, C. She, J. M. Szarko, L. X. Chen, and J. T. Hupp, "Dye-sensitized solar cells: sensitizer-dependent injection into ZnO nanotube electrodes," *Langmuir,* vol. 26, pp. 1401-1404, 2009.
[6] H. J. Snaith and C. Ducati, "$SnO_2$-based dye-sensitized hybrid solar cells exhibiting near unity absorbed photon-to-electron conversion efficiency," *Nano letters,* vol. 10, pp. 1259-1265, 2010.
[7] K. Hara, T. Horiguchi, T. Kinoshita, K. Sayama, H. Sugihara, and H. Arakawa, "Highly efficient photon-to-electron conversion with mercurochrome-sensitized nanoporous oxide semiconductor solar cells," *Solar Energy Materials and Solar Cells,* vol. 64, pp. 115-134, 2000.
[8] S. Yang, H. Kou, H. Wang, K. Cheng, and J. Wang, "Preparation and band energetics of transparent nanostructured $SrTiO_3$ film electrodes," *The Journal of Physical Chemistry C,* vol. 114, pp. 815-819, 2009.
[9] B. Tan, E. Toman, Y. Li, and Y. Wu, "Zinc stannate ($Zn_2SnO_4$) dye-sensitized solar cells," *Journal of the American Chemical Society,* vol. 129, pp. 4162-4163, 2007.
[10] E. Meagher, C. Schwerdtfeger, and M. Horn, "Golden Book of Phase Transitions," ed: Wroclaw, 2002.

©IJRASET (UGC Approved Journal): All Rights are Reserved

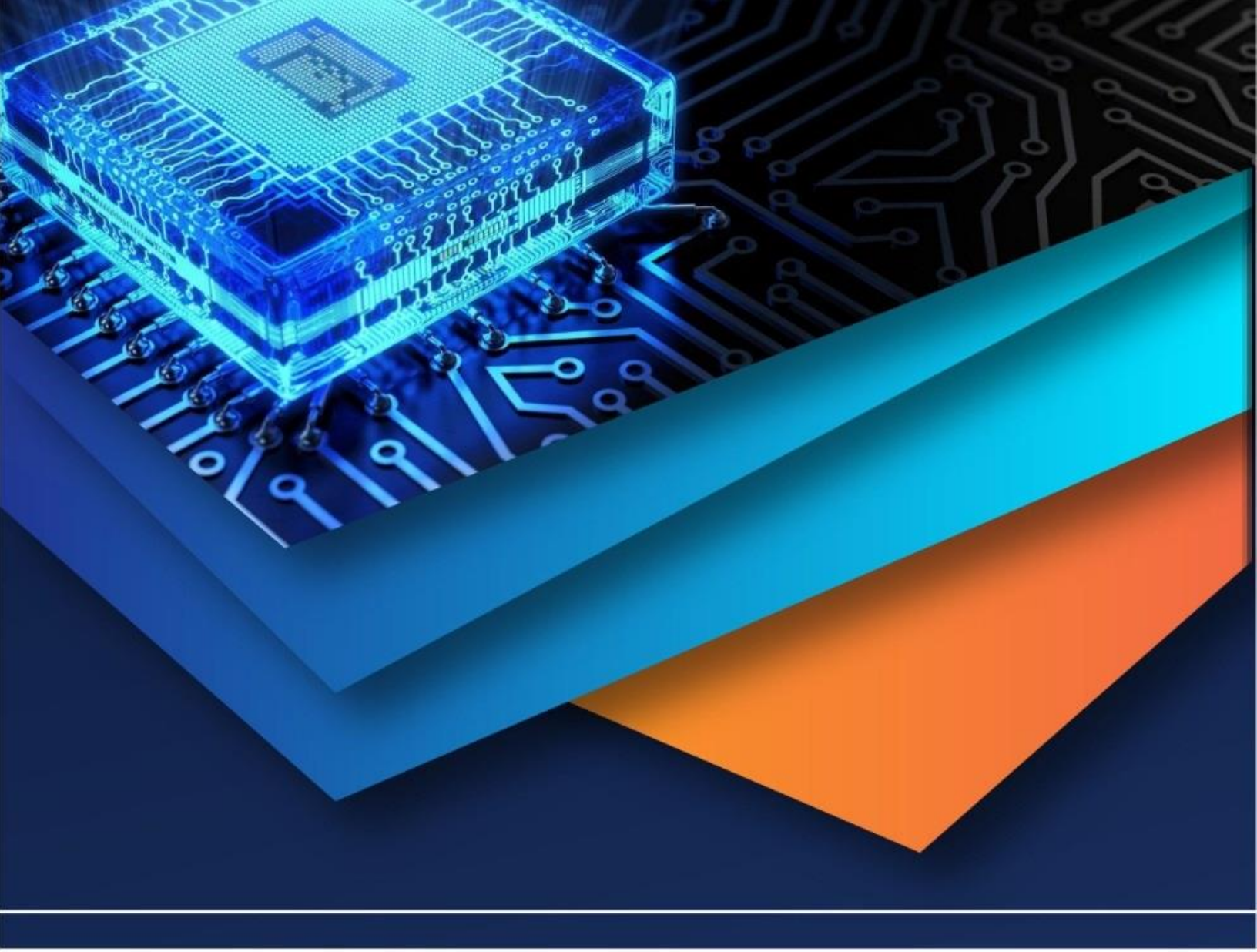

10.22214/IJRASET

45.98

IMPACT FACTOR: 7.129

IMPACT FACTOR: 7.429

# INTERNATIONAL JOURNAL FOR RESEARCH

IN APPLIED SCIENCE & ENGINEERING TECHNOLOGY

Call : 08813907089 (24*7 Support on Whatsapp)